

Bottleneck Accumulation of Hybrid Magnetoelastic Bosons

Dmytro A. Bozhko,^{1,2,*} Peter Clausen,¹ Gennadii A. Melkov,³ Victor S. L'vov,⁴ Anna Pomyalov,⁴
Vitaliy I. Vasyuchka,¹ Andrii V. Chumak,¹ Burkard Hillebrands,¹ and Alexander A. Serga¹

¹*Fachbereich Physik and Landesforschungszentrum OPTIMAS, Technische Universität Kaiserslautern, 67663 Kaiserslautern, Germany*

²*Graduate School Materials Science in Mainz, Kaiserslautern 67663, Germany*

³*Faculty of Radiophysics, Electronics and Computer Systems, Taras Shevchenko National University of Kyiv, Kyiv 01601, Ukraine*

⁴*Department of Chemical Physics, Weizmann Institute of Science, Rehovot 76100, Israel*

(Received 7 February 2017; published 8 June 2017)

An ensemble of magnons, quanta of spin waves, can be prepared as a Bose gas of weakly interacting quasiparticles. Furthermore, the thermalization of the overpopulated magnon gas through magnon-magnon scattering processes, which conserve the number of particles, can lead to the formation of a Bose-Einstein condensate at the bottom of a spin-wave spectrum. However, magnon-phonon scattering can significantly modify this scenario and new quasiparticles are formed—magnetoelastic bosons. Our observations of a parametrically populated magnon gas in a single-crystal film of yttrium iron garnet by means of wave-vector-resolved Brillouin light scattering spectroscopy evidence a novel condensation phenomenon: A spontaneous accumulation of hybrid magnetoelastic bosonic quasiparticles at the intersection of the lowest magnon mode and a transversal acoustic wave.

DOI: 10.1103/PhysRevLett.118.237201

Macroscopic quantum states—Bose-Einstein condensates (BECs) can be created in overpopulated gases of bosonic quasiparticles (excitons [1], polaritons [2–4], magnons [5–8], photons [9], etc.). However, interactions between quasiparticles of a different nature [10], for example, between magnons and phonons in a magnetic medium [11–18], can significantly alter the properties of these gases and thus modify the condensation scenarios [19,20]. Here, we report on the discovery of a novel condensation phenomenon mediated by the magnon-phonon interaction: A bottleneck accumulation of hybrid magnetoelastic bosons. We have found that the transfer of quasiparticles toward a BEC state is almost fully suppressed near the intersection point between the magnon and phonon spectral branches. Such a bottleneck leads to a strong spontaneous accumulation of the quasiparticles trapped near the semilinear part of the magnon-phonon hybridization area. As opposed to BEC, which is a consequence of equilibrium Bose statistics, the bottleneck accumulation is determined by varying interparticle interactions. Furthermore, unlike BEC, the accumulated magnetoelastic bosons possess a nonzero group velocity, making them promising data carriers in prospective magnon spintronics [21] circuits.

The energy spectra of an overpopulated magnon-phonon gas were studied at room temperature in an yttrium iron garnet (YIG, $\text{Y}_3\text{Fe}_5\text{O}_{12}$) film by frequency-, time- and wave-vector-resolved Brillouin light scattering (BLS) spectroscopy [22,23] [see Fig. 1(a)]. Following the approach, which was established in previous experiments on a magnon BEC [6–8], magnons were injected into the

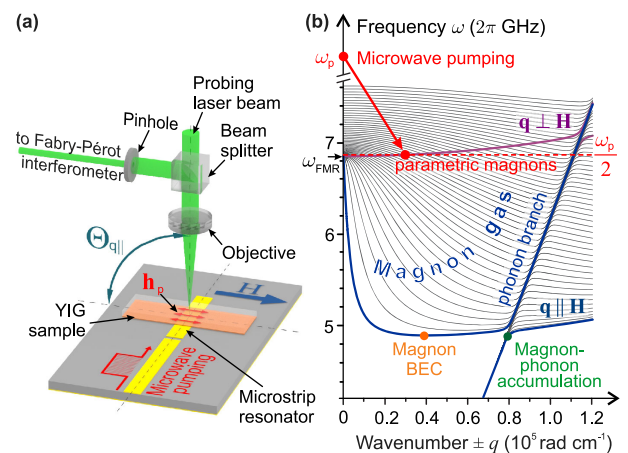


FIG. 1. (a) Schematic illustration of the experimental setup. The resonator concentrates the applied microwave energy and induces a pumping microwave Oersted field h_p oriented along the bias magnetic field \mathbf{H} , thus realizing conditions for the parallel parametric pumping. The probing laser beam is focused onto a YIG film placed on top of the microstrip resonator. The light inelastically scattered by magnons is redirected to a Fabry-Pérot interferometer for frequency and intensity analysis. Wave-number-selective probing of magnons with wave vectors $\mathbf{q} \parallel \mathbf{H}$ is realized by varying the incidence angle $\Theta_{q \parallel}$ between the field \mathbf{H} and the probing laser beam. (b) Magnon-phonon spectrum of a $6.7 \mu\text{m}$ -thick YIG film calculated for $H = 1735 \text{ Oe}$. 47 thickness modes with $\mathbf{q} \parallel \mathbf{H}$ are shown. The upper thick curve shows the most effectively parametrically driven [26] lowest magnon mode with $\mathbf{q} \perp \mathbf{H}$. The arrow illustrates the magnon injection to the frequency $\omega_p/2$ slightly above the ferromagnetic resonance frequency ω_{FMR} .

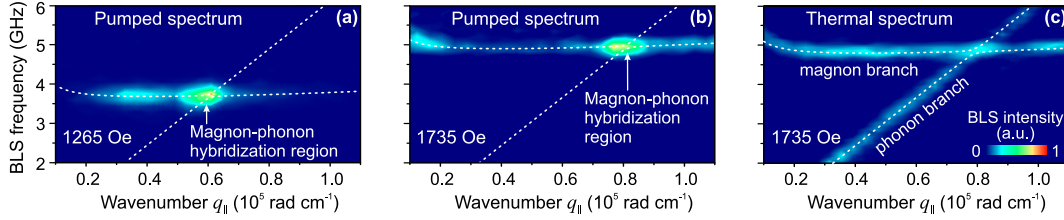


FIG. 2. Magnon-phonon spectra and their population under different pumping conditions. White dashed lines represent the calculated dispersion relation for the lowest magnon branch ($\mathbf{q} \parallel \mathbf{H}$), hybridized with a transversal acoustic mode. Strong population of the magnon-phonon hybridization region is clearly visible in the parametrically pumped spectra (a)–(b) measured in the case of a $500 \mu\text{m}$ -wide pumping area. The width of the population peak is of the order of the wave number resolution of the experimental setup, i.e., $\pm 0.02 \times 10^5 \text{ rad cm}^{-1}$. No distinct peculiarities in the thermal spectrum measured for zero pump power are detected (c).

in-plane magnetized YIG film via parallel parametric pumping [24]. In this process, one photon of a pumping electromagnetic field of frequency ω_p splits into two magnons having opposite wave vectors $\pm \mathbf{q}$ and frequency $\omega_p/2$ [see the red arrow in Fig. 1(b)]. Single-crystal YIG is a ferrimagnetic insulator that combines the uniquely low magnon and phonon damping [25] with a pronounced nonlinear magnon dynamics thus allowing for an efficient thermalization of externally injected magnons. This thermalization causes an increase in the chemical potential of the pumped magnon gas, and when it becomes equal to the minimum magnon energy a magnon BEC forms at this spectral point [see Fig. 1(b)] [6,7].

Surprisingly, by virtue of the wave-vector-resolved BLS technique we have detected another spectral point where the quasiparticles accumulate away from the global energy minimum of a pure magnon spectrum [compare the orange and green dots in Fig. 1(b)]. BLS intensity maps representing the population of the magnon-phonon spectrum are presented in Figs. 2(a) and 2(b) as a function of frequency and wave number q_{\parallel} ($\mathbf{q} \parallel \mathbf{H}$) for two different bias magnetic fields and a relatively small pumping power P_p of 2.6 W. In spite of the fact that the threshold for magnon BEC formation is still not reached at such power levels, one can see an intense population peak near the region of the hybridization between the magnon and the transversal acoustic phonon dispersion branches (see white lines in Fig. 2). As the bias magnetic field is shifted from 1265 Oe to 1735 Oe, the population peak shifts in frequency and wave number together with the magnetoelastic crossover region. At the same time, there are no peculiarities in the thermal spectrum, measured at the same conditions, but without the application of pumping [see Fig. 2(c)].

It is important that the population peak is visible only if a sufficiently wide microstrip resonator is used to create the pumping microwave field h_p [see Fig. 1(a)]. This then confirms that the accumulation occurs into the magnon-phonon hybridization region, where quasiparticles possess rather high group velocities—the widening of the width of the microstrip reduces their leakage from the pumping area. Obviously, the accumulation mechanism must significantly differ from the conventional BEC as no energy minimum exists in this region.

To reveal characteristic features of the observed accumulation effect, we performed time-resolved BLS measurements for both the narrow ($50 \mu\text{m}$) and the wide ($500 \mu\text{m}$) pumping areas. The results are presented in Fig. 3. Evidently, there is a delay between the application of the pumping pulse and the population of the lowest energy states of the spin-wave spectrum by thermalized magnons. In both cases [Figs. 3(a), 3(b)], this delay is determined by two contributions. The first contribution is the time required for the parametric process to develop. The second one is the time needed for the injected parametric magnons to scatter to the bottom of the spectrum, where first magnons are detected in the exchange region of the spectrum at the maximal detectable wave number value of $q_{\parallel} = 1.1 \times 10^5 \text{ rad cm}^{-1}$. The total delay depends on the density of the pumping microwave field and, thus, is slightly different for Figs. 3(a) and 3(b) because of the different resonator widths. Then, a pronounced population peak is formed at the magnetoelastic crossover at $q_{\parallel} = 0.8 \times 10^5 \text{ rad cm}^{-1}$ in the case of the wide pumping area [see Fig. 3(a)]. On the contrary, in compliance with our previously reported results [7,27], no accumulation is visible in this spectral region in the case of the narrow pumping area [see Fig. 3(b)]. During further time evolution, the magnons occupy energy states around the global energy minimum $q_0 = 0.4 \times 10^5 \text{ rad cm}^{-1}$ and tend to form a Bose-Einstein condensate. The intensification of the spectral flow of gaseous magnons to the global energy minimum in a freely evolving magnon gas leads to the appearance of the BEC's density peak [7] and to the slight increase in the density of the accumulated magnetoelastic quasiparticles just after the termination of the pumping pulse.

Remarkably, the magnetoelastic peak emerges at pumping powers at least ten times smaller than the threshold of the BEC formation [see the right panel of Fig. 3(a)]. Nevertheless, with the increase of the pumping power (and consequently of the BEC density), further growth in the population of the magnetoelastic peak is suppressed [see black and red lines in the right panel of Fig. 3(a)].

To understand the observed phenomena, we should consider the peculiarities of the scattering processes leading to the thermalization of the parametrically driven magnon gas. A microwave electromagnetic field with frequency ω_p

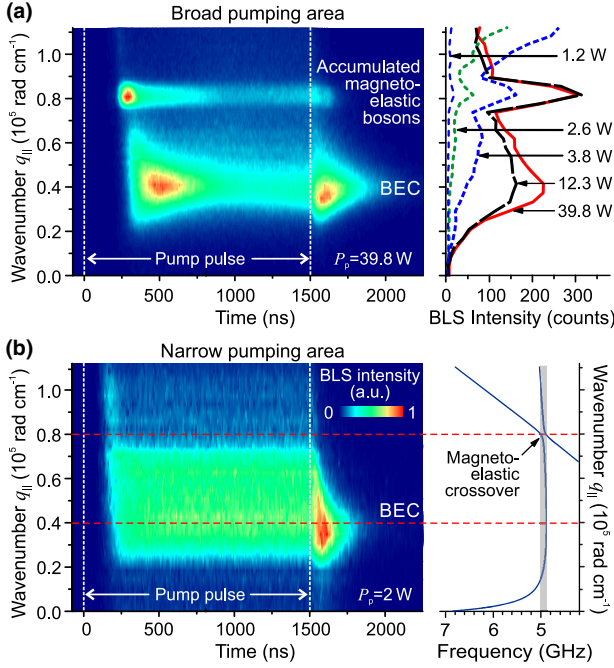


FIG. 3. Temporal dynamics of the magnon gas density. (a) Pronounced accumulation of magnetoelastic bosons is evident for the broad pumping area of $500 \mu\text{m}$ width. The right panel shows the pumping power dependencies of the quasiparticle density integrated by time. The saturation of the magnetoelastic peak at high pumping powers argues in favor of a relationship between the magnon BEC and the accumulation phenomenon. No accumulation effect is visible in (b) due to a strong leakage of fast magnetoelastic bosons from the narrow pumping area of $50 \mu\text{m}$ width. The pumping power is significantly decreased due to the increase in the density of a microwave current in the narrow microstrip. In all measurements BLS data are collected in the frequency band of 150 MHz near the bottom of the magnon spectrum [see the shaded area in the right panel of (b)]. The bias magnetic field is $H = 1735 \text{ Oe}$.

and wave number $q_p \approx 0$ excites parametric magnons, distributed over the isofrequency surface $\omega_{\mathbf{q}}^m = \omega_p/2$ [see Fig. 1(b)]. The essential part of these magnons possesses wave numbers belonging to the exchange region of the spectrum, where “ $2 \Rightarrow 2$ ” four-magnon scattering with the laws of conservation $\omega_{\mathbf{q}_1}^m + \omega_{\mathbf{q}_2}^m = \omega_{\mathbf{q}_3}^m + \omega_{\mathbf{q}_4}^m$ and $\mathbf{q}_1 + \mathbf{q}_2 = \mathbf{q}_3 + \mathbf{q}_4$ dominates over other types of interactions. This interaction redistributes the parametrically excited magnons over the entire \mathbf{q} space, such that the flux of the magnon number $n(\mathbf{q})$ is mostly directed toward lower frequencies. To find the fastest track in the \mathbf{q} space for magnons flowing from the pumping area toward the BEC destination point, we note that at relatively high frequencies, the main contribution to the scattering amplitude $T_{\mathbf{q}_1, \mathbf{q}_2; \mathbf{q}_3, \mathbf{q}_4}$ is given by the exchange interactions for which $T_q \equiv T_{\mathbf{q}, \mathbf{q}; \mathbf{q}, \mathbf{q}} \propto q^2$ (see, e.g., Ref. [28]). Therefore, the magnons with the largest wave numbers q are most efficiently thermalized. For an in-plane magnetized YIG film, they belong to the lowest magnon mode with $\mathbf{q} \parallel \mathbf{H}$ [27,29]. Thus, the fastest way for the parametric magnons

from the pumping area toward the bottom of the energy well lies along the dispersion curve of this mode.

In the presence of magnon-phonon coupling, the unperturbed magnon $\omega_{\mathbf{q}}^m$ and phonon $\omega_{\mathbf{q}}^p$ spectra [see Fig. 4(a), dashed lines] split up into upper and lower magnetoelastic modes (U-MEM, $\Omega_{\mathbf{q}}^U$ and L-MEM, $\Omega_{\mathbf{q}}^L$), [Fig. 4(a), solid lines]. The population dynamics of these modes are determined by both the intramodal ($2L \Leftrightarrow 2L$, $2U \Leftrightarrow 2U$) and the intermodal ($2L \Leftrightarrow 2U$) scattering of hybrid magnetoelastic bosons with the scattering amplitudes $T_{q_1, q_2; q_3, q_4}^{LL}$, $T_{q_1, q_2; q_3, q_4}^{UU}$ and $T_{q_1, q_2; q_3, q_4}^{LU}$, respectively. Notice that nonlinear interaction between phonons is much weaker than that for magnons (see, e.g., Refs. [24,25,28]) and can be peacefully ignored in the problem at hands. The same can be stated about the process of magnon-phonon scattering, which originates from relativistic spin-orbit interaction and is very weak in YIG [24,25]. Therefore, the only nonlinear scattering process that must be taken into account is the exchange four-magnon scattering described by the amplitudes $T_{q_1, q_2; q_3, q_4}$. As a result, all above-mentioned magnetoelastic scattering amplitudes are proportional to the magnon contribution to MEMs. It can be shown (see, e.g., Chap. I in Ref. [28] and in more details in Ref. [30]) that this contribution is given by $\cos \varphi_q$ for the L-MEM and $\sin \varphi_q$ for the U-MEM, whose values are determined by the dimensionless frequency distance o_q from the crossover:

$$\cos \varphi_q = \frac{1}{\sqrt{2}} \left(1 + \frac{o_q}{\sqrt{1 + o_q^2}} \right)^{1/2}, \quad o_q = \frac{\omega_q^p - \omega_q^m}{\Delta}, \quad (1)$$

where $\Delta = \Omega_{\mathbf{q}_x}^U - \Omega_{\mathbf{q}_x}^L$ is the magnetoelastic frequency and \mathbf{q}_x is the crossover wave vector, at which $\omega_{\mathbf{q}_x}^p = \omega_{\mathbf{q}_x}^m \equiv \omega_{\mathbf{q}_x}$ [Fig. 4(a)]. In particular,

$$T_q^{LL} = T_q \cos^4 \varphi_q, \quad T_q^{LU} = T_q \cos^2 \varphi_q \sin^2 \varphi_q, \quad (2)$$

and $T_q^{UU} \approx T_q \sin^4 \varphi_q$. Plots of T_q^{LL} , T_q^{UU} , and T_q^{LU} vs o_q are shown in Fig. 4(b). As expected, for positive o_q (i.e., $q > q_x$), the L-MEM becomes a pure magnon mode with $T_q^{LL} \rightarrow T_q$, while the U-MEM becomes a pure phonon mode with $T_q^{UU} \rightarrow 0$ [see Figs. 4(a) and 4(b)]. The intermodal amplitude T_q^{LU} [shown by a red solid line in Fig. 4(b)] requires the presence of the magnon contribution in both the L- and U-MEMs; therefore, its value is significant only in the hybridization region, where $|o_q| \lesssim 1$.

A consistent description of the evolution of a parametrically driven magnon system towards BEC, including bottleneck accumulation of the L-MEM population around the hybridization area, may be achieved in the framework of the weak wave turbulence theory [31], further developed in Ref. [28] to describe the spin-wave turbulence under parametric excitation. The main tool of this theory is a kinetic equation for the occupation numbers $n(\mathbf{q})$ of waves [in our case, $n^L(\mathbf{q})$ and $n^U(\mathbf{q})$ of L- and U-MEMs]. However, such a kinetic-equation-based description for

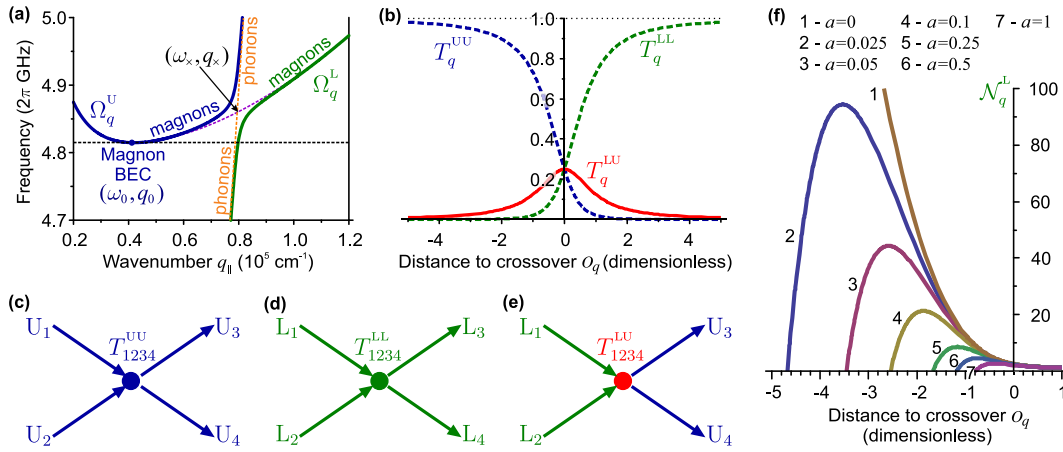


FIG. 4. Theory of the bottleneck accumulation. (a) Calculated magnon-phonon spectrum near the hybridization region. (b) Interaction amplitudes T_q^{UU} , T_q^{LL} , and T_q^{LU} , normalized by T_q , vs the dimensionless distance from the hybridization crossover o_q . (c)–(e) Schematic representation of the scattering and cross-scattering four-particle processes in the hybridization region. (f) Solutions of the dimensionless L-MEM density \mathcal{N}_q^L , for different values of the parameter a .

the actual YIG frequency spectra and the interaction amplitudes is beyond the scope of this Letter. Here, we aim at a quantitative understanding of this problem (under the simplifying assumption of spherical symmetry) by reducing the kinetic equation for $n^L(q)$ to the stationary balance equation for the one-dimensional density of L-MEM quasiparticles $N_q^L = 4\pi q^2 n^L(q)$. This equation can be written as follows:

$$\frac{d\mu_q^L}{dq} = F_q^{LU}. \quad (3)$$

Here, μ_q is the L-MEM flux towards the hybridization area, originating from the intramodal $2L \Rightarrow 2L$ scattering, conserving the total number $\int N_q^L dq$ of L-MEM quasiparticles, while F_q^{LU} is the transport rate $N_q^L \rightarrow N_q^U$, caused by the intermodal $2L \Rightarrow 2U$ scattering. Using the kinetic equation for $n^L(\mathbf{q})$ [28,30,31], we estimated μ_q and F_q^{LU} in the vicinity of the hybridization as

$$\begin{aligned} \mu_q^L &\approx q_x^3 (T_q^{LL})^2 (N_q^L)^3 \omega_x^{-1}, \\ F_q^{LU} &\approx q_x^2 (T_q^{LU})^2 (N_q^L)^2 N_q^U \omega_x^{-1}. \end{aligned} \quad (4)$$

Here N_q^U is the one-dimensional density of U-MEMs at sufficiently large negative o_q , say at $o_q \approx -5$. Using these estimates we rewrite the balance Eq. (3) as

$$\frac{d}{dq} [\cos^8 \varphi_q (\mathcal{N}_q^L)^3] = 3a (\mathcal{N}_q^L)^2 \cos^4 \varphi_q \sin^4 \varphi_q. \quad (5)$$

Here, $\mathcal{N}_q^L = N_q^L / N_+^L$ is the dimensionless L-MEM density, normalized by the density N_+^L at a sufficiently large positive o_q , say at $o_q \approx +5$. The parameter $a = bN_-^U / N_+^L$ involves a dimensionless coefficient b (presumably of the order of unity), which combines all the uncontrolled parameters in our estimates.

The ordinary differential equation (5) can be solved with the boundary condition $\lim_{q \rightarrow \infty} \mathcal{N}_q^L = 1$, giving the relative MEMs population in the hybridization region

$$\mathcal{N}_q^L = \frac{1}{\cos^{8/3} \varphi_q} \left[1 - a \int_q^\infty \frac{\sin^4 \varphi_p dp}{\cos^{4/3} \varphi_p} \right]. \quad (6)$$

Solutions of Eq. (6) for different values of a [Fig. 4(f)], exhibit a sharp rise in the L-MEM population, caused by the bottleneck accumulation of MEM bosons near the hybridization region. The maximum possible (asymptotic) bottleneck with an infinite growth of $\mathcal{N}_q^L \propto |q|^{-8/3}$ for large negative o_q corresponds to the case where $a = 0$, in which only the intramodal scattering, conserving the total number of L-MEMs, is accounted for. For finite a , this growth is suppressed by the intermodal scattering that transfers quasiparticles from the L-MEM to the U-MEM. When this transfer is small ($a \ll 1$), the L-MEM density accumulation is quite significant, while for large $a \approx 1$ [see two lower lines in Fig. 4(f) for $a = 1$ and 0.5] there is practically no MEM accumulation. Importantly, the increase in the population of the U-MEM during the course of the BEC formation (i.e., increase in N_-^U and, as a consequence, in a) must lead to the suppression of the bottleneck effect and to the consequent saturation of the MEM population peak. This effect is clearly visible in our observations shown in Fig. 3(a).

The distance in the phase space between the BEC and MEM areas can be easily varied by the change of a bias magnetic field [see Figs. 2(a), 2(b)], potentially allowing the control of the dynamics of magnon condensates and supercurrents [8] by the adjustment of their incoherent and coherent intermodal scattering with magnetoelastic bosons. It should be noted that according to our theory and in contrast to BEC, represented by a single macroscopic mode [8,32,33], the bottleneck accumulation occurs in a narrow but finite spectral region. Although the theory describes the accumulation of

turbulent waves, it does not prohibit the formation of a coherent state in a cloud of accumulated quasiparticles. The possibility of a coherent dynamics constitutes an intriguing problem of fundamental importance for physics in general and for forthcoming magnonic applications.

The bottleneck accumulation phenomenon, reported here for a magnon-phonon gas, is not unique for this particular system and can occur in any multicomponent gas mixture of interacting quasiparticles with significantly different scattering amplitudes. For example, the accumulation of magnetic polaritons [34] is expected in out-of-plane magnetized ferrimagnetic films. Similar effects can potentially occur in an exciton-polariton system in semiconductor microcavities [35], and in hybrids of coupled atomic condensates and microwave radiation in binary ultracold bosonic gases [36,37]. It is necessary to note that the reported bottleneck phenomenon exclusively relates to the variable scattering interaction of quasiparticle *hybrids* and, thus, should not be mixed with a “bottleneck” in a relaxation chain from an externally excited quasiparticle state to the phonon bath [38]. In our case, the latter effect is a prerequisite for an increase in the density of externally pumped gaseous magnons above the thermal level.

Financial support from the Deutsche Forschungsgemeinschaft (project INST 161/544-3 within the Transregional Collaborative Research Centre SFB/TR 49 “Condensed Matter Systems with Variable Many-Body Interactions”), from EU-FET (Grant InSpin 612759) and from the State Fund for Fundamental Research of Ukraine (SFFR) is gratefully acknowledged. D. A. B. was supported by a fellowship of the Graduate School Material Sciences in Mainz (MAINZ) through DFG funding of the Excellence Initiative (GSC-266). As well we acknowledge I.I. Syvorotka (Scientific Research Company “Carat”, Lviv, Ukraine) for supplying us with the YIG film sample.

*bozhko@physik.uni-kl.de

- [1] L. V. Butov, A. L. Ivanov, A. Imamoglu, P. B. Littlewood, A. A. Shashkin, V. T. Dolgoplov, K. L. Campman, and A. C. Gossard, *Phys. Rev. Lett.* **86**, 5608 (2001).
- [2] J. Kasprzak, M. Richard, S. Kundermann, A. Baas, P. Jeambrun, J. M. J. Keeling, F. M. Marchetti, M. H. Szymańska, R. André, J. L. Staehli, V. Savona, P. B. Littlewood, B. Deveaud, and Le Si Dang, *Nature (London)* **443**, 409 (2006).
- [3] R. Balili, V. Hartwell, D. Snoke, L. Pfeiffer, and K. West, *Science* **316**, 1007 (2007).
- [4] S. R. K. Rodriguez, J. Feist, M. A. Verschuuren, F. J. Garcia Vidal, and J. Gómez Rivas, *Phys. Rev. Lett.* **111**, 166802 (2013).
- [5] A. S. Borovik-Romanov, Yu. M. Bun'kov, V. V. Dmitriev, and Yu. M. Mukharskiĭ, *JETP Lett.* **40**, 1033 (1984).
- [6] S. O. Demokritov, V. E. Demidov, O. Dzyapko, G. A. Melkov, A. A. Serga, B. Hillebrands, and A. N. Slavin, *Nature (London)* **443**, 430 (2006).
- [7] A. A. Serga, V. S. Tiberkevich, C. W. Sandweg, V. I. Vasyuchka, D. A. Bozhko, A. V. Chumak, T. Neumann, B. Obry, G. A. Melkov, A. N. Slavin, and B. Hillebrands, *Nat. Commun.* **5**, 3452 (2014).
- [8] D. A. Bozhko, A. A. Serga, P. Clausen, V. I. Vasyuchka, F. Heussner, G. A. Melkov, A. Pomyalov, V. S. L'vov, and B. Hillebrands, *Nat. Phys.* **12**, 1057 (2016).
- [9] J. Klaers, J. Schmitt, F. Vewinger, and M. Weitz, *Nature (London)* **468**, 545 (2010).
- [10] L. Venema, B. Verberck, I. Georgescu, G. Prando, E. Couderc, S. Milana, M. Maragkou, L. Persechini, G. Pacchioni, and L. Fleet, *Nat. Phys.* **12**, 1085 (2016).
- [11] K. Uchida, H. Adachi, T. An, T. Ota, M. Toda, B. Hillebrands, S. Maekawa, and E. Saitoh, *Nat. Mater.* **10**, 737 (2011).
- [12] M. Agrawal, V. I. Vasyuchka, A. A. Serga, A. D. Karenowska, G. A. Melkov, and B. Hillebrands, *Phys. Rev. Lett.* **111**, 107204 (2013).
- [13] A. Rückriegel, P. Kopietz, D. A. Bozhko, A. A. Serga, and B. Hillebrands, *Phys. Rev. B* **89**, 184413 (2014).
- [14] S. M. Rezende, R. L. Rodríguez-Suárez, J. C. Lopez Ortiz, and A. Azevedo, *Phys. Rev. B* **89**, 134406 (2014).
- [15] J. Flipse, F. K. Dejene, D. Wagenaar, G. E. W. Bauer, J. B. Youssef, and B. J. van Wees, *Phys. Rev. Lett.* **113**, 027601 (2014).
- [16] S. R. Boona and J. P. Heremans, *Phys. Rev. B* **90**, 064421 (2014).
- [17] K. An, K. S. Olsson, A. Weathers, S. Sullivan, X. Chen, X. Li, L. G. Marshall, X. Ma, N. Klimovich, J. Zhou, L. Shi, and X. Li, *Phys. Rev. Lett.* **117**, 107202 (2016).
- [18] T. Kikkawa, K. Shen, B. Flebus, R. A. Duine, K. I. Uchida, Z. Qiu, G. E. W. Bauer, and E. Saitoh, *Phys. Rev. Lett.* **117**, 207203 (2016).
- [19] J. Hick, T. Kloss, and P. Kopietz, *Phys. Rev. B* **86**, 184417 (2012).
- [20] S. A. Bender, R. A. Duine, A. Brataas, and Y. Tserkovnyak, *Phys. Rev. B* **90**, 094409 (2014).
- [21] A. V. Chumak, V. I. Vasyuchka, A. A. Serga, and B. Hillebrands, *Nat. Phys.* **11**, 453 (2015).
- [22] O. Büttner, M. Bauer, S. O. Demokritov, B. Hillebrands, Y. S. Kivshar, V. Grimalsky, Y. Rapoport, and A. N. Slavin, *Phys. Rev. B* **61**, 11576 (2000).
- [23] C. W. Sandweg, M. B. Jungfleisch, V. I. Vasyuchka, A. A. Serga, P. Clausen, H. Schultheiss, B. Hillebrands, A. Kreisel, and P. Kopietz, *Rev. Sci. Instrum.* **81**, 073902 (2010).
- [24] A. G. Gurevich and G. A. Melkov, *Magnetization Oscillations and Waves* (CRC Press, Boca Raton, 1996).
- [25] V. Cherepanov, I. Kolokolov, and V. L'vov, *Phys. Rep.—Rev. Sec. Phys. Lett.* **229**, 81 (1993).
- [26] A. A. Serga, C. W. Sandweg, V. I. Vasyuchka, M. B. Jungfleisch, B. Hillebrands, A. Kreisel, P. Kopietz, and M. P. Kostylev, *Phys. Rev. B* **86**, 134403 (2012).
- [27] D. A. Bozhko, P. Clausen, A. V. Chumak, Yu. V. Kobljanskyj, B. Hillebrands, and A. A. Serga, *Low Temp. Phys.* **41**, 801 (2015).
- [28] V. S. L'vov, *Wave Turbulence Under Parametric Excitations (Applications to Magnetics)* (Springer, New York, 1994).
- [29] P. Clausen, D. A. Bozhko, V. I. Vasyuchka, B. Hillebrands, G. A. Melkov, and A. A. Serga, *Phys. Rev. B* **91**, 220402(R) (2015).

- [30] D. A. Bozhko, P. Clausen, G. A. Melkov, V. S. L'vov, A. Pomyalov, V. I. Vasyuchka, A. V. Chumak, B. Hillebrands, and A. A. Serga, [arXiv:1612.05925](https://arxiv.org/abs/1612.05925).
- [31] V. E. Zakharov, V. S. L'vov, and G. E. Falkovich, *Kolmogorov Spectra of Turbulence (Wave Turbulence)* (Springer, New York, 1992).
- [32] P. Nowik-Boltyk, O. Dzyapko, V. E. Demidov, N. G. Berloff, and S. O. Demokritov, *Sci. Rep.* **2**, 482 (2012).
- [33] O. Dzyapko, P. Nowik-Boltyk, B. Koene, V. E. Demidov, J. Jersch, A. Kirilyuk, T. Rasing, and S. O. Demokritov, *IEEE Magn. Lett.* **7**, 3501805 (2016).
- [34] M. I. Kaganov, N. B. Pustyl'nik, and T. I. Shalaeva, *Phys. Usp.* **40**, 181 (1997).
- [35] T. Byrnes, N. Y. Kim, and Y. Yamamoto, *Nat. Phys.* **10**, 803 (2014).
- [36] J. Qin, G. Dong, and B. A. Malomed, *Phys. Rev. Lett.* **115**, 023901 (2015).
- [37] J. Qin, G. Dong, and B. A. Malomed, *Phys. Rev. A* **94**, 053611 (2016).
- [38] A. S. Borovik-Romanov and N. M. Kreines, *Phys. Rep.* **81**, 351 (1982).